

Multicolor CCD Photometry of the Dusty, Giant, Late-Type Spiral Galaxy NGC 5351

A. S. Gusev¹ and S. S. Kaĭsin²

¹*Sternberg Astronomical Institute, Universitetskii pr. 13, Moscow, 119992 Russia*

²*Special Astrophysical Observatory, Russian Academy of Sciences,
Nizhniĭ Arkhyz, Želenchuk, Karachaevo-Cherkesiya 369167, Russia*

Received April 21, 2003; in final form, March 15, 2004

Abstract—The paper reports the results of *BVRI* surface photometry of the giant galaxy NGC 5351 based on CCD observations obtained on the 1-m telescope of the Special Astrophysical Observatory of the Russian Academy of Sciences. Analysis of the structure and radial brightness distribution in the galaxy shows that NGC 5351 has a complex and, in some places, asymmetric structure. The galaxy possesses a large quantity of dust. The average internal extinction due to dust is $A_V = 1.2^m \pm 0.4^m$. After correcting for the effect of this dust, the parameters of the galaxy are typical of late-type spirals. The compositions of the stellar population in various parts of the galaxy are estimated using two-color diagrams. Star-forming regions in NGC 5351 are identified and studied. Most of the star-forming regions are located in the ring of the galaxy. Evolutionary modeling is used to estimate the ages of regions of violent star formation. An elliptical companion galaxy to NGC 5351 was found. The rotation curve of the galaxy is modeled and its mass estimated. The disk of NGC 5351 is self-gravitating within its optical radius.

© 2004 MAIK “Nauka/Interperiodica”.

1. GENERAL INFORMATION

The giant and fairly distant barred spiral galaxy NGC 5351 (Fig. 1) remains a comparatively poorly studied object. Table 1 gives the principal parameters of the galaxy according to the RC3 catalog [1]. Various authors have estimated the position angle of the galaxy within a radius of $\sim 1'$ from the nucleus to be from 93° [2] to 104° [3].

Photometry of the galaxy has been performed in the *V* [4], *R* [3, 5, 6], and *V* and *I* [7] filters. However, so far, no detailed multicolor photometry has been carried out for NGC 5351. According to [3–6], the brightness of the galactic disk decreases exponentially with distance on a scale of about $20''$.

The galaxy has a regular, symmetrical shape; its two spiral arms wind up, forming an inner ring. Numerous long and continuous outer arms extend outside the ring [2, 8, 9]. NGC 5351 has a small companion—the galaxy NGC 5349—located $3.4'$ to the southeast [2].

21-cm HI observations revealed a powerful gaseous disk extending to 1.5 optical radii of the galaxy [10]. The gas motions in some local regions of the outer disk and in the spiral arms of the galaxy are strongly perturbed [2]. Given the accepted distance of 48.9 Mpc, the mass of the galaxy within $1'$ from the center is estimated to be $2.2 \times 10^{11} M_\odot$ [2, 10],

and the mass of HI, to be $1.3 \times 10^{10} M_\odot$ [10]. The integrated mass-to-luminosity ratio is $M/L = 6.5(M/L)_\odot$ [2]. A rotation curve for NGC 5351 can be found in [2].

2. OBSERVATIONS AND DATA REDUCTION

We observed NGC 5351 on January 21–22 and 22–23, 1998, with the 1-m Zeiss-1000 telescope (focal distance 13.3 m) of the Special Astrophysical Observatory of the Russian Academy of Sciences equipped with a standard CCD photometer [11]. The K585 CCD camera combined with *B*, *V*, *R*, and *I* broadband filters realizes a photometric system that is close to the standard Johnson–Cousins *BVRI* system. The 530×580 pixels CCD yields a $143'' \times 212''$ field of view for an image scale of $0.28'' \times 0.37''$ per pixel. Table 2 gives information about the observations.

We took five to six exposures in each filter, shifting the telescope by several arcseconds between each exposure to reduce the effect of CCD defects. The seeing was $2.5''$ – $3.5''$.

The photometric calibration of the galaxy was based on standard stars (PG 0220, PG 1407, RU 149, and S 101429) from the list of Majewski *et al.* [12] observed on the same night. We also used the aperture photometry data for the galaxy from [13].

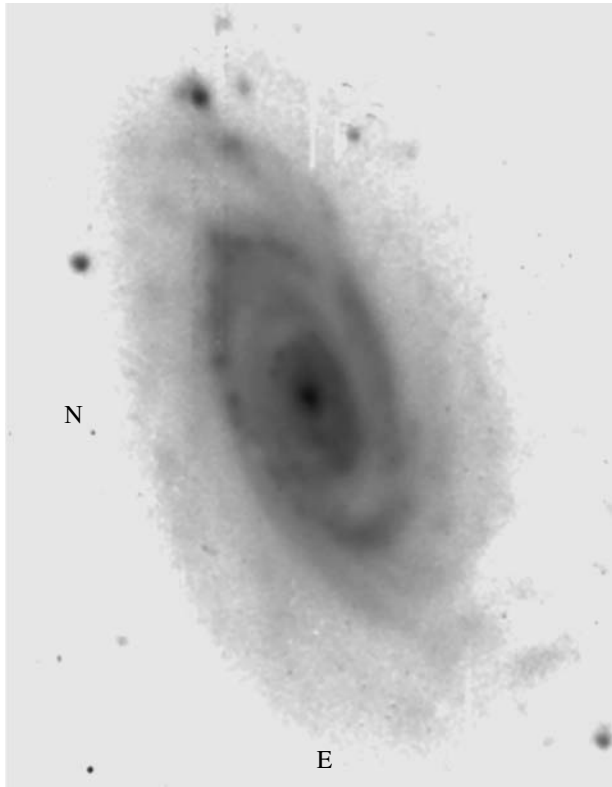


Fig. 1. CCD R image of NGC 5351. The size of the image is $2.4' \times 3.5'$.

The accuracy of the photometric calibration was 0.12^m , 0.08^m , 0.05^m , and 0.04^m in B , V , R , and I , respectively. The errors of the photometric measurements of the galaxy reported below in Section 3 do not include these calibration errors, which must be added to the errors listed in Section 3 to obtain the absolute photometric errors. This is not true, however, for the photometric data for the companion galaxy NGC 5351 (see Section 3.4 and Table 5 below); in

this case, the corresponding errors include the photometric calibration errors.

We performed the preliminary reduction of the images at the Special Astrophysical Observatory of the Russian Academy of Sciences. To correct for electron bias and the effect of “hot pixels” and bad columns of the CCD array, we subtracted a dark frame that was the average of several exposures taken with a closed shutter and the same integration time as for the object. We used summed frames of the twilight sky with signal-to-noise ratios of no less than 60 to 80 taken in each of the filters as flat fields. We divided each image by its flat field to correct for the nonuniform sensitivity of the detector pixels.

We performed the subsequent data reduction at the Sternberg Astronomical Institute using a standard procedure incorporating the ESO MIDAS image processing procedures. The principal reduction stages included the following.

(a) Scaling of the images to $0.37''/\text{pixel}$ and alignment of the galaxy images (with an accuracy of up to 0.1 pixel). The alignment of the images made it possible to efficiently eliminate cosmic-ray traces and the effects of individual hot pixels and bad columns of the CCD.

(b) Determining the sky background and subtracting it from each frame.

(c) Coadding the galaxy images taken in the same filters.

(d) Correcting for the air mass.

(e) Transforming the counts to a logarithmic scale ($\text{mag}/\text{arcsec}^2$) based on the results of the photometric calibration.

(f) Reducing the instrumental photometric system to the standard Johnson–Cousins photometric system (taking into account the derived color equations).

(g) Subtracting galaxy images taken in different filters in order to obtain color-index maps.

Table 1. Principal parameters of NGC 5351

Parameter	Value
Type	SBb
m_B , mag	13.00
$M_B^{0,i}$, mag	-21.19
V_{LG} , km/s	3667
R , Mpc ($H_0 = 75 \text{ km s}^{-1} \text{ Mpc}^{-1}$)	48.9
D_{25} , arcmin	2.88
i , deg	59.2
PA, deg	100

Table 2. Log of observations

Date	Filter	Exposures, s
Jan. 21–22, 1998	B	3×600
	V	4×600
	R	4×600
	I	4×600
Jan. 22–23, 1998	B	2×600
	V	2×600
	R	1×600
	I	1×600

We also used images of NGC 5351 in the J , H , and K IR filters taken from the 2MASS catalog. We reduced these images using a procedure similar to that applied to the optical frames. The JHK images have a seeing of $1''$ and a scale of $1.0''/\text{pixel} \times 1.0''/\text{pixel}$.

We corrected all the data (brightness and color indices) for Galactic extinction (based on the RC3 data). When constructing two-color diagrams and investigating the color characteristics of sites of star formation, we also corrected for extinction associated with the inclination of the disk of NGC 5351 (based on the RC3 data). In the latter case, the corrected quantities are marked by the subscripts “0, i .” Table 3 lists the adopted corrections for the various filters. The image scale is $88 \text{ pc}/\text{pixel}$ for the accepted distance of the galaxy.

3. ANALYSIS OF THE RESULTS

3.1. Photometric Profiles and Morphology of the Galaxy

The galaxy has a diffuse, moderately bright nuclear region: the maximum brightness within several pixels of the nucleus exceeds $\mu_V = 19.6^m/\text{arcsec}^2$ (Fig. 2a). The diameter of the nucleus— 3.2 kpc ($14''$; Figs. 2a and 2b)—is fairly large, but we should bear in mind that NGC 5351 is a large galaxy (according to [1], its diameter is 41 kpc). The isophotes are much less flattened in the nucleus than in the disk (especially in the IR), and their ellipticity reaches $e = 0.17$ in the I filter (Fig. 3a), indicating the presence of an extended bulge whose flux predominates in the central region (within $10''$). The position angle of the isophotes varies as a function of the wavelength (from 136° in B to 101° in I , see Fig. 3b).

The $8.3 \text{ kpc} \times 5.2 \text{ kpc}$ ($35'' \times 22''$) central region of the disk of NGC 5351, whose isophotes are extended along the major axis of the galaxy, is of special interest. The isophotes in this region are nearly rectangular (see the $21.5^m/\text{arcsec}^2$ isophote in Fig. 2b), and the region itself is shifted to the east of the nucleus (see the asymmetry of the photometric profiles at nucleocentric distances of $7''$ – $20''$ in Fig. 2a). This region morphologically resembles an asymmetric bar. We show below that the asymmetry of the bar is due to the nonuniform distribution of dust in the galaxy. The B and V surface brightnesses of the bar to the west of the nucleus do not vary with distance and are equal to $20.8 \pm 0.2^m/\text{arcsec}^2$ in V (Fig. 2a). In the redder filters (R and, especially, I), the brightness decreases with galactocentric distance (e.g., from 19.2 to $19.7^m/\text{arcsec}^2$ in I), reflecting the known fact that the fraction of young stars increases toward the tip of the bar [14].

Table 3. Galactic extinction and extinction due to the inclination of NGC 5351

Color index	E	$E(i)$
$B-V$	0.06	0.09
$V-R$	0.03	0.05
$R-I$	0.04	0.07

The observed structure of the bar east of the nucleus is complex: it has a semiring with a radius of 1.9 kpc ($8''$; Fig. 1) whose V brightness is 0.1^m – $0.15^m/\text{arcsec}^2$ higher than the brightness of the surrounding background. A short (in projection) spiral arm winding in the direction opposite to that of other arms emerges from the tip of the eastern part of the bar. However, in this case, we may be observing a disconnected ring (Figs. 1 and 2b). This is the brightest arm in the galaxy, and its surface brightness reaches $\mu_V = 21.3 \pm 0.1^m/\text{arcsec}^2$. Afanas'ev *et al.* [2] pointed out the presence of strongly noncircular gas motions in this region. The ellipticity of the bar isophotes is $e = 0.20 \pm 0.05$ in B , V , and R and somewhat higher in I (Fig. 3a). The position angle of the bar is $105.5^\circ \pm 0.5^\circ$ in V , R , and I (Fig. 3b).

The inner spiral arms of the galaxy, which form a ring with a diameter of 17.5 kpc ($74''$), are barely visible against the disk. Only the western inner arm is conspicuous (Fig. 1). Figure 2a clearly shows the arrangement of the arms: the section made through the northwestern part of NGC 5351 ($r = -40''$ to $-20''$) passes nearly along the western spiral arm ($\mu_V = 21.65 \pm 0.15^m/\text{arcsec}^2$), while the section made through the southeastern part of the galaxy ($r = 20''$ – $40''$) crosses the inner disk ($\mu_V = 22.1 \pm 0.2^m/\text{arcsec}^2$) and ring (the maximum $\mu_V = 21.2^m/\text{arcsec}^2$).

Two spiral arms can be seen in the outer disk of NGC 5351, in the western and eastern parts of the galaxy. A bright diffuse object is visible at the tip of the western arm (Figs. 1 and 2b). See Section 3.4 for a more detailed discussion of this object.

The position angle of the galaxy can be very accurately determined from the orientation of its outer isophotes: $\text{PA} = 111.2^\circ \pm 0.6^\circ$. The inclination of the disk inferred from the flattening of the B , V , and R isophotes of the thick disk is $i = 62^\circ \pm 1^\circ$. I images of the galaxy yield a somewhat higher inclination, $i = 65^\circ$. Figure 4 shows averaged photometric profiles of NGC 5351 computed for the derived PA and i . The region of the ring of the galaxy is prominent at $r = 37''$ and separates the galactic disk into its inner and outer parts.

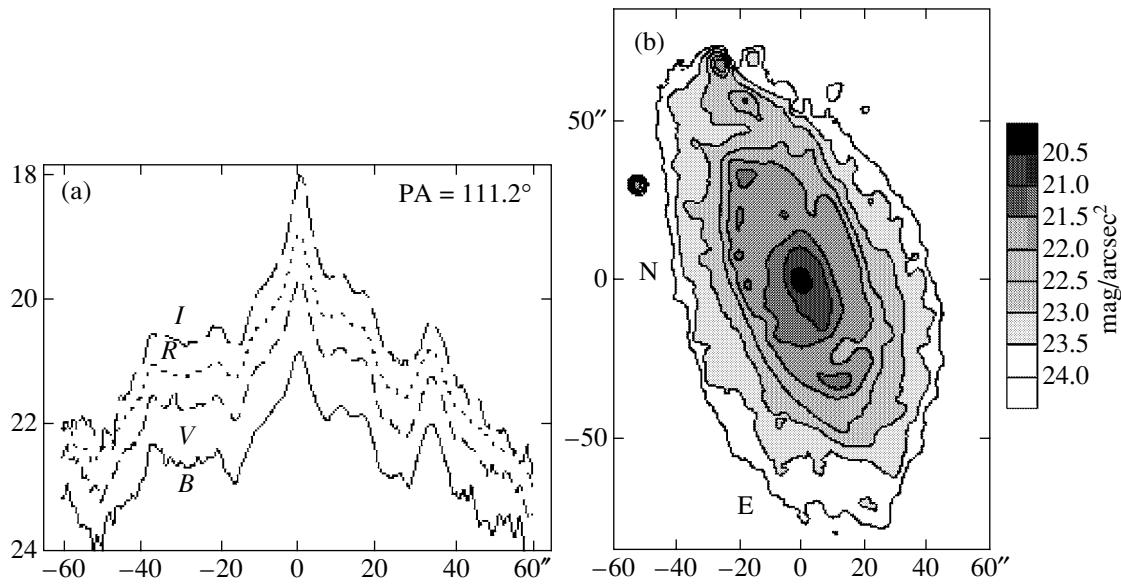


Fig. 2. (a) Photometric profiles along the major axis of NGC 5351 (in $\text{mag}/\text{arcsec}^2$) taken in the B (solid), V (short-dashed), R (dotted), and I (long-dashed) filters, and (b) the V image of the galaxy.

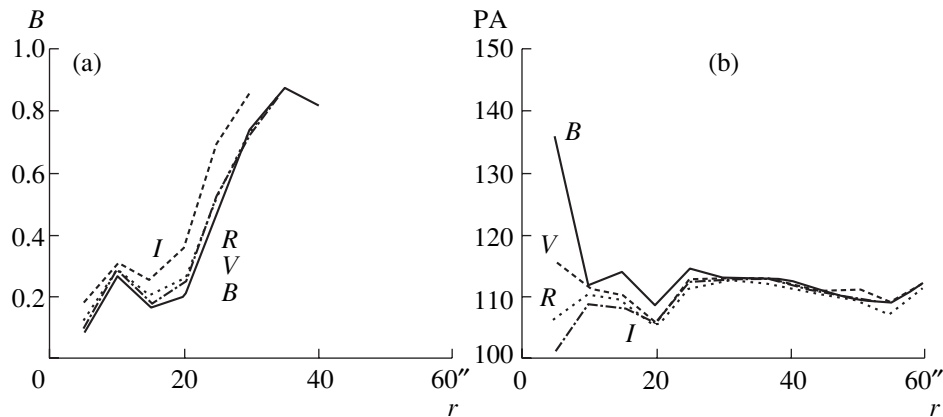


Fig. 3. (a) Isophote ellipticity $e = 1 - b/a$ and (b) position angle of the galaxy in B , V , R , and I as functions of distance r from the center of NGC 5351.

Analysis of the brightness profiles showed that the inner and outer parts of the disk have different parameters and that this difference becomes more pronounced at shorter wavelengths. The brightness of the outer disk ($r = 50'' - 70''$) decreases exponentially on a scale of 6.79 ± 0.17 kpc ($28.6'' \pm 0.7''$) in V and 5.25 ± 0.39 kpc ($22.2'' \pm 1.7''$) in K . The central brightnesses are $\mu_V = 20.78 \pm 0.20^m/\text{arcsec}^2$ and $\mu_K = 17.32 \pm 0.09^m/\text{arcsec}^2$ in V and K , respectively. The brightness in the region $r = 12'' - 28''$ occupied by the inner disk decreases exponentially in a somewhat steeper fashion, on a scale of 4.60 ± 0.24 kpc ($19.4'' \pm 1.0''$) in V and 4.60 ± 0.08 kpc ($19.4'' \pm 0.3''$) in K . The corresponding central brightnesses are $\mu_V = 20.23 \pm 0.27^m/\text{arcsec}^2$ and $\mu_K =$

$16.83 \pm 0.06^m/\text{arcsec}^2$ (without subtracting the parameters of the outer disk). The I and K brightnesses of the outer disk decrease faster than the brightness in bluer filters (B , V , and R), probably due to an increase in the number of hot, young stars toward the periphery of the galaxy. On the other hand, the scale length of the inner disk is virtually the same in all filters, which suggests the absence of a young stellar population in this region of the galaxy.

A decomposition of the central region of the galaxy into the inner disk and bulge shows that the brightness decreases in accordance with a de Vaucouleurs law at galactocentric distances $r = 2'' - 8''$. The bulge has effective radius $r_e(V) = 2.6 \pm 0.6$ kpc ($10.8'' \pm 2.6''$), $r_e(K) = 1.6 \pm 1.0$ kpc ($6.5'' \pm 4.2''$),

$\mu_V(r_e) = 26.65 \pm 1.15^m/\text{arcsec}^2$, and $\mu_K(r_e) = 22.91 \pm 1.48^m/\text{arcsec}^2$. We thus conclude that the spherical component (bulge) contributes negligibly to the total luminosity and mass of the galaxy: the luminosity of the bulge is $3.5 \pm 2.0\%$ of the total K luminosity of NGC 5351.

3.2. Distribution of Colors and Dust

On the whole, NGC 5351 is as a rather red galaxy—its integrated color index is $B-V = 0.8^m$ [1]. Such $B-V$ values are typical of S0 galaxies. However, we show below that the galaxy contains a large quantity of dust; the reddening of the galaxy due to selective extinction by dust is, on average, $E(B-V) \sim 0.4^m$. It follows that the integrated $B-V$ color index of NGC 5351 is 0.4^m , which is typical of Sc galaxies. The intrinsic color indices of various parts of the galaxy will also be smaller than their observed values (by $0.3^m-0.7^m$ for $B-V$).

The nucleus of NGC 5351 is redder than the galaxy as a whole; its color indices are $B-V = 1.10^m \pm 0.05^m$ and $V-R = 0.57^m \pm 0.03^m$ (Figs. 5a–5c). The nucleus is especially prominent in $R-I$ (Figs. 5a and 5d). The color of the galaxy becomes bluer with distance from the nucleus—all three color indices decrease with galactocentric distance ($B-V$ from $1.05^m \pm 0.10^m$ to $0.7^m \pm 0.1^m$, $V-R$ from $0.65^m \pm 0.05^m$ to $0.4^m \pm 0.1^m$, and $R-I$ from $0.9^m \pm 0.1^m$ to $0.3^m \pm 0.2^m$). Figure 5a shows the clear asymmetry of the color parameters of NGC 5351 to the west and east of the nucleus at galactocentric distances ranging from $5''$ to $35''$. This asymmetry can be explained by the complex morphology of the galaxy in this region: to the west of the nucleus ($r = -5''$ to $35''$), the section passes through the inner spiral arm, while the section to the east of the nucleus ($r = 5''-35''$) passes through the bar and inner disk.

As we noted in Section 3.1, the bar of the galaxy becomes bluer toward its periphery. Its color indices decrease from $0.96^m \pm 0.01^m$ to $0.86^m \pm 0.01^m$ in $B-V$, from $0.63^m \pm 0.01^m$ to $0.40^m \pm 0.01^m$ in $V-R$, and from $0.68^m \pm 0.02^m$ to $0.60^m \pm 0.02^m$ in $R-I$ (Fig. 5a). The color indices of the western inner spiral arm coincide with the corresponding mean color indices of the bar. As a result, the color-index contours in Fig. 5b ($B-V = 0.9^m$, $V-R = 0.50^m$, and $R-I = 0.55^m$) bound a region whose shape resembles that of a standard symmetrical bar. This indicates that the stellar population of the bar is the same as that of the western spiral arm (i.e., the region located within 5.6 kpc ($20''$) of the center).

The ring of NGC 5351 is bluer than the surrounding regions of the outer and inner disks. This is especially obvious in Fig. 5a at $r = \pm 35''$ (where the section intersects the ring). The color indices of the

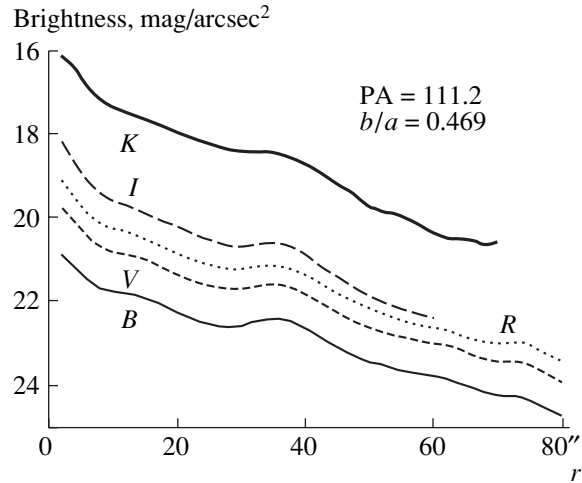


Fig. 4. Averaged B , V , R , I , and K photometric profiles of NGC 5351 (in $\text{mag}/\text{arcsec}^2$).

ring, $B-V = 0.75^m \pm 0.04^m$ and $V-R = 0.35^m \pm 0.03^m$, are $0.1^m-0.2^m$ smaller than the corresponding color indices of the surrounding regions. The brightest parts of the ring are clearly visible in Figs. 5b and 5c, but the ring cannot be distinguished in $R-I$ (Fig. 5a), suggesting a similarity between the old stellar populations of the disk and galactic ring.

The $R-I$ color index decreases much faster along the minor axis than do $B-V$ and $V-R$ (Fig. 5d). The integrated IR color indices of the galaxy are $J-H = 0.68^m$ and $H-K = 0.25^m$.

We used the BVK images of the galaxy to estimate the distribution of dust and the extinction it produces in the galaxy. We applied the technique and model computations of Rhee and Albada [15], developed for the analysis of the distribution of internal extinction in a galaxy based on the $(B-V)_0-(V-K)_0$ two-color diagram. Figure 6 shows the distributions of dust and the associated extinction in NGC 5351. Note that the distribution of the internal extinction depends strongly on the adopted model for the composition of the stellar population, the star-formation history, and the distribution of the dust with respect to the stellar disk and is therefore only approximate. The derived extinctions A_V are accurate to $\pm 0.35^m$. For regions of ongoing star formation with an extremely young stellar population, A_V can be calculated unambiguously using the $(B-V)_0-(V-K)_0$ diagram. We analyze the extinction in star-forming regions in Section 3.4 and do not show this in Fig. 6.

Analysis of the distribution of dust yields some insights into the morphology of the galaxy. The nonuniform dust distribution in the central region of NGC 5351 explains the asymmetry of the bar (Fig. 2a). The numerous dust lanes in the disk distort its structure (in its northern and southeastern parts)

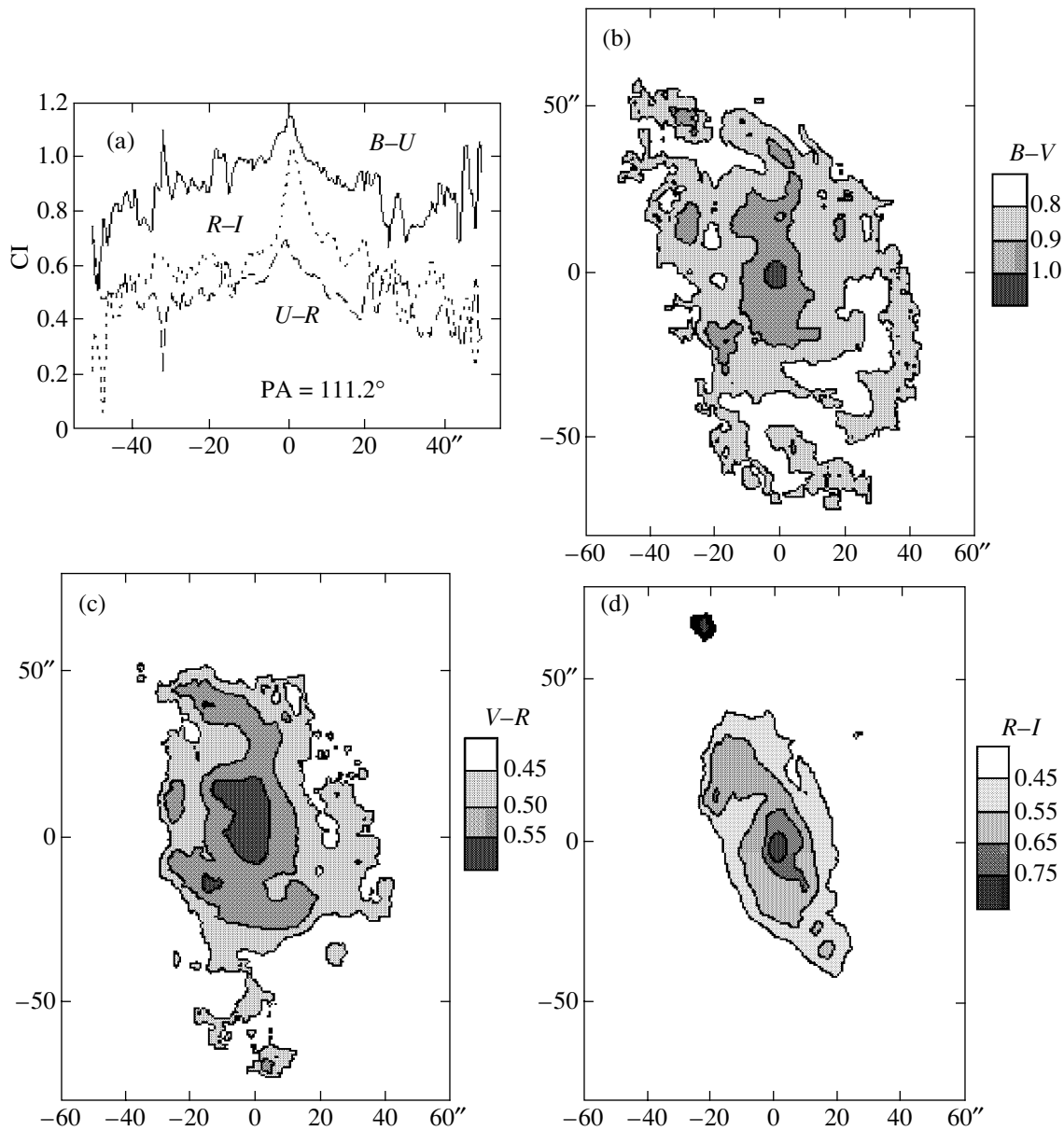


Fig. 5. (a) $B-V$ (solid), $V-R$ (dashed), and $R-I$ (dotted) color indices measured along the major axis of NGC 5351 and maps of the (b) $B-V$, (c) $V-R$, and (d) $R-I$ color indices.

and the spiral arms of the galaxy (in the northern, western, and southeastern parts of the galaxy). This all suggests that the observed “irregularity” of the structure of NGC 5351 can be explained by the nonuniform distribution of dust in the galaxy.

The B , V , and K photometric parameters of the galaxy can be used to estimate the internal extinction by dust, which proves to be fairly strong: $A_V = 1.2^m \pm 0.35^m$, on average, for the entire galaxy, with A_V increasing from 0.6^m in the central region to 2.1^m in the dust lanes of the outer disk and regions of ongoing star formation. These extinctions correspond to reddenings $E(B-V) = 0.2^m - 0.7^m$. We

have $E(B-V) = 0.4^m \pm 0.1^m$, on average, for the entire galaxy. It follows that the intrinsic color of NGC 5351 is typical of late-type spiral galaxies. The strong internal extinction of the galaxy explains the discrepancy between its observed color parameters (typical of early-type galaxies) and the lack of an appreciable bulge (a characteristic feature of late-type galaxies).

3.3. Two-Color Diagrams

Figures 7a–7d show the $(B-V)_0^i - (V-R)_0^i$ and $(B-V)_0^i - (R-I)_0^i$ two-color diagrams for various regions of NGC 5351. The numbers in Figs. 7a and

7c indicate the colors of 1 the nucleus within $4''$ of the center; 2 the bulge at galactocentric distances of $4''-7''$; 3 the spiral arms; 4, 5 the inner and outer disks, respectively; and 6–8 the bar at galactocentric distances of 1.3, 2.4, and 3.8 kpc ($5.5''$, $10''$, and $16''$), respectively.

The two-color diagrams have been corrected for extinction due to the inclination of NGC 5351, so that the color indices for different regions differ somewhat from those obtained in Section 3.2. The differences between the corresponding color indices—the reddening due to the inclination of NGC 5351—are given in Table 3.

The color indices are not corrected for the internal extinction by dust in the galaxy we have estimated here. Extinction by dust cannot explain the deviations of points in the diagrams from the normal integrated color sequence of galaxies (NCS); it shifts points upward and to the left along the NCS.

The points representing the color indices of different regions of the galaxy are aligned along a line that does not coincide with the NCS. The galactocentric distances of regions are correlated fairly well with their positions on the two-color diagrams: regions are shifted increasingly to the left and upward with increasing galactocentric distance (Figs. 7a and 7c). This behavior indicates an increase in the fraction of young stars toward the periphery of the galaxy. A number of regions are located to the left of the NCS, which cannot be explained by the effect of dust or the specific nature of the chemical composition of the galaxy, since these factors would shift points nearly along the NCS in the $(B-V)_0^i - (V-R)_0^i$ and $(B-V)_0^i - (V-I)_0^i$ diagrams. The regions in question are mostly in the outer parts of the bar. Their deviation from the NCS may be a consequence of a complex star-formation history in the disk of NGC 5351. The shift of points representing the color indices of the bar to the left of the NCS may be due to a deficit of intermediate-age stars in the outer parts of the bar [14]. The circumnuclear region of NGC 5351 occupies a position in the two-color diagrams that corresponds to systems with old stellar populations (with ages of about 10^{10} yr).

3.4. Star-Forming Regions and the Companion Galaxy

Nine small and mostly blue starlike and diffuse bright regions have been identified in NGC 5351. The color indices of a bright starlike object to the north of NGC 5351 (Figs. 1 and 2b) identified it as a field star, and we do not analyze this object below. Figures 7b and 7d show the positions of the remaining eight objects on the two-color diagrams. Table 4 lists the

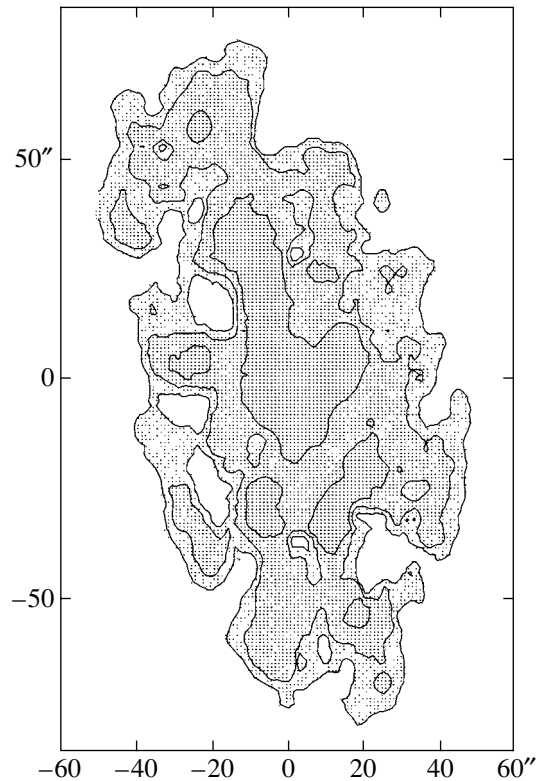


Fig. 6. Map of internal extinction by dust A_V in NGC 5351. Extinction contours are shown at 1.0^m , 1.5^m , and 2.0^m . Lighter regions correspond to stronger extinction.

derived parameters of these regions: (1) the number of the object; (2) coordinates of the region in arcsec relative to the center of the galaxy; (3–5) $(B-V)_0^i$, $(V-R)_0^i$, and $(V-I)_0^i$ color indices; (6) the diameter of the object in pc; and (7) the age of the object. We determined the diameter of each region from the best-quality V frame (with $2.1''$ seeing, which corresponds to 500 pc). We determined the brightness of the regions studied in each filter by subtracting the brightness of the surrounding base of NGC 5351 from the brightness distribution of the region occupied by the object. We inferred the ages of the regions from their positions on the two-color diagrams using evolutionary tracks of aging stellar systems computed with the PEGASE2 program developed by Fioc and Rocca-Volmerange (Institut d'Astrophysique de Paris) [17]. The color indices of the stellar systems were modeled using the initial mass function of Kennicutt with upper and lower mass limits of $120 M_\odot$ and $0.1 M_\odot$. We considered systems with metallicities Z higher and lower than the solar value.

Five diffuse objects (2–4, 6, and 7) are located in the ring of NGC 5351. Four are located in the northern part of the ring (2–4, and 7), have characteristic sizes ranging from 650 to 1350 pc (so that these

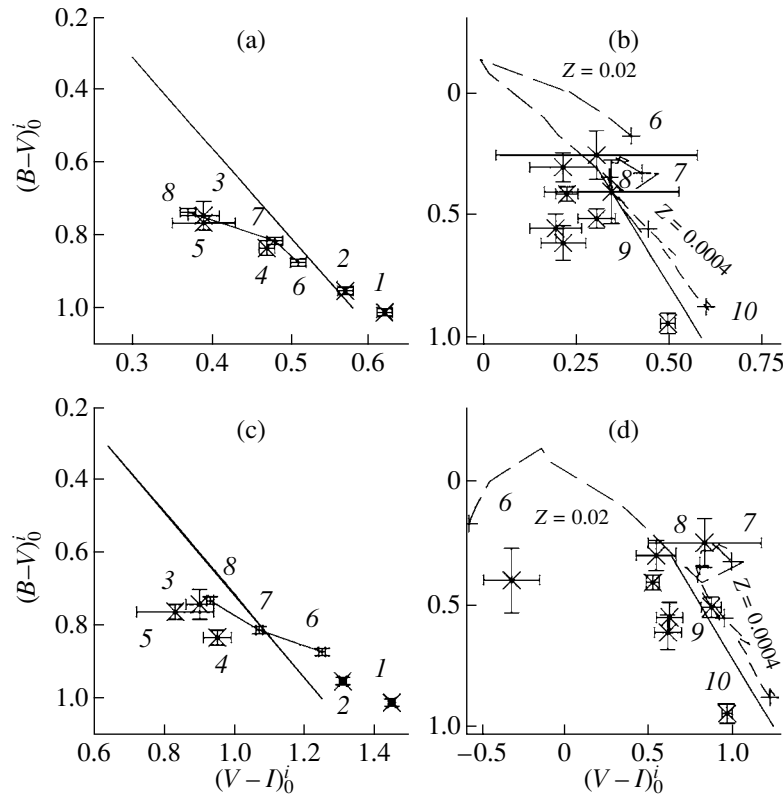


Fig. 7. (a, b) $(B-V)_0 - (V-R)_0$ and (c, d) $(B-V)_0 - (V-I)_0$ two-color diagrams for (a, c) NGC 5351 and (b, d) sites of star formation in the galaxy. The straight solid line shows the NCS of galaxies according to Buta and Williams [16]. The solid broken lines in diagrams (a, c) show the variation of the color indices along the major axis of the bar in NGC 5351. The dashed lines in diagrams (b, d) show the evolutionary tracks of an aging stellar system in which all its stars formed in a single burst of star formation during the first 10^6 yr at $Z = 0.02$ for an age of $10^6 - 5 \times 10^8$ yr (long-dashed line) and at $Z = 0.0004$ for an age of $5 \times 10^8 - 2 \times 10^{10}$ yr (short-dashed line). The numbers in diagrams (b, d) indicate the logarithm of the age of the system (in yr). Also shown are the errors. See text for other notation.

objects are stellar complexes in the classification of Efremov [18]), and are located somewhat to the left of the NCS and below the evolutionary tracks. Object 1, which is in the outer western spiral arm, has similar parameters. Such strong deviations of the positions of these regions from the evolutionary tracks in the diagrams can be explained only by very strong selective extinction by dust (the reddening $E(B-V)$ inside the regions may reach $0.6^m - 0.7^m$ for objects 3 and 7). This ties in with the results we obtained in Section 3.2. Extinction by dust shifts points downward and to the right along the NCS [16] in the two-color diagrams. In this case, all the objects considered here are young star-forming regions with ages of the order of $(3-8) \times 10^6$ yr and extinctions by dust of $\sim 1^m - 2^m$ in V (Figs. 7b and 7d).

Region 6, which is located in the southern part of the ring, has color indices that are typical of a very young stellar system with an age of $< 3.2 \times 10^6$ yr (Figs. 7b and 7d). This region has a diameter of 1 kpc, implying that it is a stellar complex in the classification of Efremov.

Object 5, which is located to the south of the nucleus in the region occupied by the bar, is of considerable interest. It is a compact object with a diameter of less than 500 pc. The large errors of the measured color indices prevent a confident determination of its age, but its position in the two-color diagrams indicates that this region should be populated by moderately young stars.

The position of the bright diffuse object at the western edge of the outer disk of NGC 5351 (at a deprojected galactocentric distance of $73''$ (17.5 kpc)) in the two-color diagrams indicates an old composition for its stellar population. A bar emerging from the disk of the galaxy toward this region can be seen in Figs. 1 and 2b. The photometric parameters of the object are consistent with the colors of a globular cluster, but its size (3.4 kpc) exceeds the typical sizes of globular clusters by almost two orders of magnitude. If this object has a metal-poor stellar population (by analogy with globular clusters), its age is about 10^{10} yr for $Z = 0.0004 - 0.004$. The absolute magnitude of the object is $M_V^0 = -16.16^m \pm 0.09^m$ (for the

Table 4. Parameters of star-forming regions in NGC 5351

No.	Coordinates, arcsec	$(B-V)_0^i$	$(V-R)_0^i$	$(V-I)_0^i$	d , pc	τ , 10^6 yr
1	17.6N, 57.0W	0.41	0.22	0.53	1490	4.7 ± 0.8
2	17.2N, 0.9E	0.30	0.21	0.55	670	6.6 ± 2.8
3	20.5N, 8.2W	0.55	0.19	0.63	980	$4.5 \pm 1.3?$
4	18.7N, 31.7W	0.51	0.30	0.88	660	6.3 ± 0.7
5	5.5S, 0.6E	0.25	0.30	0.84	<500	5 – 100
6	16.1S, 0.9W	0.40	0.34	-0.32	1050	<3.2
7	11.7S, 31.4E	0.61	0.21	0.62	1350	$3.8 \pm 1.5?$

accepted distance of NGC 5351). According to the results of model computations performed using the PEGASE2 program, the object has a mass of $(1.5 \pm 1.1) \times 10^9 M_\odot$ and so must be an elliptical companion galaxy of the giant galaxy NGC 5351. In terms of its mass and photometric parameters, the object resembles the companions of M31—the elliptical galaxies NGC 147, NGC 185, and NGC 205. Table 5 gives the inferred parameters of the companion galaxy. The brightness distribution in the companion is fairly typical of small ellipticals (Fig. 8). The averaged photometric profiles of the companion galaxy can be qualitatively described by a de Vaucouleurs law with an effective radius of $2''-3''$ (0.5–0.8 kpc), which is smaller at longer wavelengths (Fig. 8). Unfortunately, a detailed analysis of the photometric parameters of this object was hindered by its small diameter, which exceeds the seeing of the images by only a modest factor. Thus, the deviation of the observed brightness distribution from a de Vaucouleurs law in the central region (Fig. 8) can be explained by “smearing” with radiation from the central region of the companion galaxy.

3.5. Rotation Curve of the Galaxy

We constructed the rotation curve of NGC 5351, $V(r)$, based on spectrophotometric observations obtained on the 6-m telescope of the Special Astrophysical Observatory [2]. Since the scatter of the data obtained by Afanas'ev *et al.* [2] is fairly large, we averaged the observed values over 2-kpc intervals (Fig. 9) before modeling the rotation curve. The last data point corresponds to the maximum rotational velocity implied by HI radio observations within a galactocentric radius of $90''$ (21.4 kpc), according to Rhee and Albada [19]. We reduced all the data to the inclination and position angle derived in Section 3.1.

The maximum of the rotation curve based on the optical data (~ 200 km/s) is located at a galactocentric distance of 9–15 kpc, which corresponds to the

radius of the ring and the outer region immediately adjacent to the ring (Section 3.1).

We modeled the rotation curve using the GR4 program developed at the Sternberg Astronomical Institute. We considered a two-component model with an exponential disk and a dark halo, with the disk scale length set equal to 6.8 kpc. We ignored the contribution of the bulge to the integrated rotation curve due to the large uncertainty in the curve.

Good agreement with the observed rotation curve can be obtained for models with various disk and halo masses. However, multicomponent models with dark halos and the minimum permissible disk mass yield unrealistically low mass-to-luminosity ratios M/L (about unity for the B and V luminosities). The observed rotation curve is fit best by a simple single-component model with a thin exponential disk (Fig. 9). The contribution of the bulge to the total

Table 5. Parameters of the companion galaxy of NGC 5351

Parameter	Value
Coordinates relative to the center of NGC 5351, arcsec	25.3N, 68.0W
Type	E3
D , kpc	3.4 ± 0.3
m_V , mag	17.29 ± 0.09
M_V^0 , mag	-16.16 ± 0.09
PA, deg	120 ± 5
$(B-V)_0$	0.94 ± 0.14
$(V-R)_0$	0.49 ± 0.10
$(V-I)_0$	0.97 ± 0.10
M/M_\odot	$(1.5 \pm 1.1) \times 10^9$
τ , yr	$\sim 10^{10}$

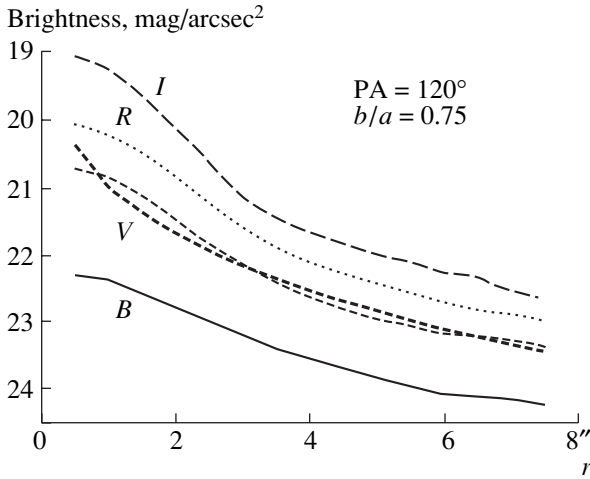


Fig. 8. Averaged B , V , R , and I photometric profiles of the companion galaxy (in $\text{mag}/\text{arcsec}^2$). The bold dashed curve shows the brightness distribution for a de Vaucouleurs law.

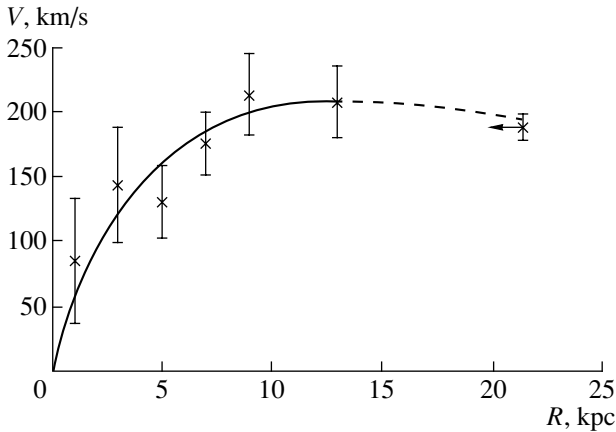


Fig. 9. Rotation curve of NGC 5351. The x's with error bars show the mean observed rotation curve based on the data of Afanas'ev *et al.* [2], with the maximum rotational velocity shown taken from Rhee and Albada [19] (the rightmost point). Also shown is the model rotation curve. All data are reduced to $\text{PA} = 111.2^\circ$ and inclination $i = 62^\circ$.

mass of the galaxy within $90''$ of its center can be assumed to be negligible in this case. The mass of the dark halo within the same radius does not exceed half of the total mass of the galaxy. It follows that the disk of NGC 5351 must be self-gravitating at these galactocentric distances.

The resulting model yielded disk masses M (which are equal to the mass of the entire galaxy) of $(1.8 \pm 0.2) \times 10^{11} M_\odot$ within $90''$ (21.4 kpc) and $(1.1 \pm 0.2) \times 10^{11} M_\odot$ within $60''$ (14.2 kpc) of the center. Given the internal extinction by dust, the luminosity of the disk within $60''$ is $L_V = (5.4 \pm 1.4) \times$

$10^{10} L_\odot$ and $L_K = (1.1 \pm 0.1) \times 10^{11} L_\odot$, and the mass-to-luminosity ratio within the same radius is $M/L_V = (2.3 \pm 1.0)(M/L_V)_\odot$, $M/L_K = (1.0 \pm 0.3)(M/L_K)_\odot$, and $M/L_B = (2.0 \pm 0.8)(M/L_B)_\odot$, respectively. These M/L values are close to those expected for galaxies with similar color parameters (according to photometric evolutionary models [20]).

NGC 5351 has the properties of a late-type spiral galaxy. Its mass-to-luminosity ratios and the model computations of the dependence of M/L on color indices reported by Bell and De Jong [20] indicate that the star-formation history in NGC 5351 is similar to that expected for late-type spiral galaxies: the star-formation rate in the galaxy decreases exponentially on a time scale of $(9 \pm 4) \times 10^9$ yr, with no powerful global bursts of star formation in the past; the metallicity of the galaxy is approximately equal to the solar value. The small contribution of the bulge to the luminosity and kinematics of the galaxy and its relative HI content are also typical of the corresponding parameters of late-type spirals. The observed red color parameters of the galaxy are due to strong internal selective extinction by dust in NGC 5351.

The only region in NGC 5351 with ongoing active processes is its ring, which divides the disk into two parts with different photometric scale lengths (Section 3.1) and hosts most of the star-forming complexes (Section 3.4) discovered so far, as well as regions of noncircular gas motions [2].

4. CONCLUSIONS

(1) We have carried out $BVRI$ CCD photometry of the giant spiral galaxy NGC 5351. The galaxy has a complex structure consisting of a bulge without a conspicuous nucleus, an inner and outer ring, an asymmetric bar, a complex spiral pattern, a disk with different color parameters inside and outside the outer ring, and numerous dust lanes.

(2) A $37''$ -radius (8.8 kpc) ring divides the disk into outer and inner parts. The V brightness of the disk ($r = 12'' - 28''$) decreases exponentially on a scale of $19.4'' \pm 1.0''$ (4.60 \pm 0.24 kpc), while that of the outer disk ($r = 50'' - 70''$) decreases exponentially on a scale of $28.6'' \pm 0.7''$ (6.79 \pm 0.17 kpc).

(3) An asymmetrical bar $35'' \times 22''$ (8.3 \times 5.2 kpc) in size can be seen. The B and V surface brightnesses of the bar to the east of the nucleus do not vary with galactocentric distance, $V = 20.8 \pm 0.2^m/\text{arcsec}^2$. The asymmetry of the bar is due to the nonuniform distribution of dust in the galaxy.

(4) The galaxy possesses large quantities of dust. The reddening of the galaxy due to selective extinction by dust is, on average, equal to $E(B-V) \sim 0.4^m$.

(5) We have identified seven starlike and diffuse star-forming regions (stellar complexes) in the galaxy. Most of these regions are located in the ring. The typical sizes and ages of the star-forming regions are 400–1350 pc and roughly $(3-8) \times 10^6$ yr.

(6) The giant elliptical galaxy NGC 5351 has a (type E3) elliptical companion galaxy to the west of its center at a distance of $73''$ (17.5 kpc). The absolute magnitude and diameter of the companion are $M_V^0 = -16.16^m \pm 0.09^m$ and 3.4 kpc.

(7) The rotation curve of NGC 5351 within $90''$ (21.4 kpc) of its center can be explained by a model with a single component—a stellar disk. The mass M of the disk in this case is $(1.8 \pm 0.2) \times 10^{11} M_\odot$. The mass and mass-to-luminosity ratios within $60''$ (14.2 kpc) of the center are $M = (1.1 \pm 0.2) \times 10^{11} M_\odot$, $M/L_V = (2.3 \pm 1.0)(M/L_V)_\odot$, and $M/L_K = (1.0 \pm 0.3)(M/L_K)_\odot$, implying that the galactic disk must be self-gravitating at the galactocentric distances considered.

(8) NGC 5351 has the properties of a late-type spiral galaxy, as is demonstrated by the small contribution of the bulge to the luminosity and kinematics of the galaxy and the relative HI content of NGC 5351. The star-formation history in the galaxy is also typical of late-type spirals: the star-formation rate decreases exponentially on a time scale of $(9 \pm 4) \times 10^9$ yr without powerful bursts of star formation in the past. The red color of the galaxy can be explained as a consequence of internal selective extinction by dust.

ACKNOWLEDGMENTS

We are grateful to A.V. Zasov (Sternberg Astronomical Institute) for sharing a model of the rotation curve of the galaxy and fruitful discussions and to D.V. Bizyaev (Sternberg Astronomical Institute) for performing the preliminary reduction of the observational data. We thank the reviewer for a number of important comments and addenda. This work was supported by the Russian Foundation for Basic Research (project nos. 01-02-16800 and 01-02-17597).

REFERENCES

1. G. de Vaucouleurs, A. de Vaucouleurs, H. G. Corwin, *et al.*, *3rd Reference Catalogue of Bright Galaxies* (Springer, New York, 1991).
2. V. L. Afanas'ev, A. N. Burenkov, A. V. Zasov, and O. K. Sil'chenko, *Astron. Zh.* **69**, 19 (1992) [*Sov. Astron.* **36**, 10 (1992)].
3. P. J. Grosbol, *Astron. Astrophys., Suppl. Ser.* **60**, 261 (1985).
4. W. E. Baggett, S. M. Baggett, and K. S. J. Anderson, *Astron. J.* **116**, 1626 (1998).
5. S. M. Kent, *Astrophys. J., Suppl. Ser.* **59**, 115 (1985).
6. S. Courteau, *Astrophys. J., Suppl. Ser.* **103**, 363 (1996).
7. J. Roth, *Astron. J.* **108**, 862 (1994).
8. D. M. Elmegreen and B. G. Elmegreen, *Astrophys. J.* **314**, 3 (1987).
9. D. M. Elmegreen and B. G. Elmegreen, *Astrophys. J.* **445**, 591 (1995).
10. A. H. Broeils and M.-H. Rhee, *Astron. Astrophys.* **324**, 877 (1997).
11. I. I. Zin'kovskii, S. S. Kaisin, A. I. Kopylov, *et al.*, *Tekh. Otchet SAO RAN* **231** (1994).
12. S. R. Majewski, R. G. Kron, D. C. Koo, and M. A. Bershad, *Publ. Astron. Soc. Pac.* **106**, 1258 (1994).
13. P. Prugniel and P. Heraudeau, *Astron. Astrophys., Suppl. Ser.* **128**, 299 (1998).
14. A. S. Gusev, *Astron. Zh.* **77**, 654 (2000) [*Astron. Rep.* **44**, 579 (2000)].
15. S. A. Kassin, J. A. Frogel, R. W. Pogge, *et al.*, *Astron. J.* **126**, 1276 (2003).
16. R. Buta and K. L. Williams, *Astron. J.* **109**, 543 (1995).
17. M. Fioc and B. Rocca-Volmerange, *Astron. Astrophys.* **326**, 950 (1997).
18. Yu. N. Efremov, *Sites of Star Formation in Galaxies* (Nauka, Moscow, 1989) [in Russian].
19. M.-H. Rhee and T. S. Albada, *Astron. Astrophys., Suppl. Ser.* **115**, 407 (1996).
20. E. F. Bell and R. S. de Jong, *Astrophys. J.* **550**, 212 (2001).

Translated by A. Dambis